RNA (1997), 3:660–676. Cambridge University Press. Printed in the USA.

The association of nonsense mutation with exon-skipping in *hprt* mRNA of Chinese hamster ovary cells results from an artifact of RT-PCR

CARRIE R. VALENTINE and ROBERT H. HEFLICH
Division of Genetic Toxicology, National Center for Toxicological Research, Jefferson, Arkansas 72079-9502, USA

ABSTRACT

RT-PCR of RNA from CHO cells with nonsense mutations in the *hprt* gene frequently detects minor *hprt* mRNA species lacking one or more exons. Many nonsense mutants also contain greatly reduced concentrations of the major, normally spliced *hprt* mRNA. In this study, we examined the hypothesis that exon-deleted mRNAs are normal constituents of CHO cells, but are not detected in wild-type parental cells and most missense mutants because their amplification is suppressed by relatively high concentrations of normally spliced *hprt* mRNA. A protocol designed to specifically detect exon-deleted mRNAs was conducted using RNA from parental cells and identified all the exon-deleted species typical of nonsense mutants. Quantitative analysis of parental cell RNA measured these exon-deleted mRNAs at ≤ 0.7% of the abundance of the full-sized species. Nonsense and missense mutants had comparable amounts of exon-deleted mRNAs, which varied both above and below parental concentrations. The relative concentrations of particular exon-deleted species could be explained by the location of nonsense mutations remaining in the mRNA or by structural effects of mutations on splicing. Exon-deleted mRNAs were detected by RT-PCR when the concentration of the most abundant exon-deleted species was ≥ 2% of the full-length mRNA. This occurred for mutants with nonsense mutations in internal exons. RT-PCR conditions were shown to suppress the amplification of exon-deleted species 40-fold when full-length mRNA was abundant, which occurred for parental lines and missense mutants. Our results verify that RT-PCR conditions can produce an artifactual association between nonsense mutation and exon-skipping when minor, exon-deleted mRNA is relatively enriched.

Keywords: mRNA abundance; quantitative RT-PCR; relative enrichment

INTRODUCTION

The hypoxanthine phosphoribosyl transferase (*hprt*) gene is one of the most widely used reporter genes for mutational analysis (Cole & Skopek, 1994). Our study of mutation in the *hprt* gene of Chinese hamster ovary (CHO) cells demonstrates that CHO cell mutants with nonsense mutations in exons 2–6 contain minor *hprt* mRNAs with deletions of exons 2, 2 and 3, and 2–4 in addition to the major, normally spliced mRNA (Manjanatha et al., 1994). These mRNA species are detected by RT-PCR (reverse transcription followed by polymerase chain reaction). Our studies also show that nonsense mutations within exons 2–7 of the CHO *hprt* gene are accompanied by a reduction in the abundance of total *hprt* mRNA to 0–30% of normal as measured by northern blot hybridization (Newton et al., 1992a; Manjanatha et al., 1994).

The association between nonsense mutation and mRNA reduction is a general phenomenon that is usually attributed to an increased degradation of mRNA [reviewed for mammalian cells by Maquat (1995, 1996) and for yeast by Caponigro and Parker (1996); Kessler and Chasin (1996)]. The reduction in mRNA abundance is limited to nonsense mutations in the internal portion of the protein-coding sequence. There is a 3′ boundary beyond which nonsense mutations have no apparent effect (Chasin et al., 1990; Cheng et al., 1990; Belgrader & Maquat, 1994; Manjanatha et al., 1994), as well as a necessary distance from the initiating AUG (Chasin et al., 1990; Manjanatha et al., 1994). In-frame exon deletions that remove a nonsense codon can result in normal levels of the exon-deleted mRNA (Belgrader et al., 1994), which then results in its enrichment relative to full-length mRNA. However, even if the deletion is out-of-frame, the frameshift could delay the appearance of a nonsense codon until it is past the 3′

Reprint requests to: Carrie R. Valentine, Division of Genetic Toxicology, National Center for Toxicological Research, HFT-120, 3900 NCTR Road, Jefferson, Arkansas 72079-9502, USA; e-mail: cvalentine@nctr.fda.gov.

boundary or could produce a nonsense codon so close to the 5′ end that it escapes the effect on mRNA abundance (mutant DU8, Chasin et al., 1990).

The generality of the association between nonsense mutation and exon-skipping is less clear. Most examples are isolated mutations from clinical specimens whose mRNA lacks only the exon that contains the nonsense mutation, rather than lacking multiple exons (Dietz et al., 1993; Gibson et al., 1993; Naylor et al., 1993; Hull et al., 1994; Will et al., 1995). Also, in contrast to our results with the *hprt* gene, most of these reports involve the efficient deletion of an exon in the major mRNA species, rather than producing a minor, exon-deleted species. However, a nonsense mutation in the gene for ornithine δ-aminotransferase does result in an exon-deleted product that is minor compared to the properly spliced species (Dietz et al., 1993). Many other nonsense mutations are not associated with exon-skipping (Maquat, 1996).

Several investigators have suggested that exon-skipping associated with nonsense mutation is a reflection of the method of semi-quantitative RT-PCR. In this relative enrichment model, exon-deleted mRNA species are normal cellular constituents, but are not detected by RT-PCR when their concentrations are low relative to the major, normally spliced mRNA (Bach et al., 1993; Gibson et al., 1993; Naylor et al., 1993; Jarolim et al., 1995; reviewed in Maquat, 1995). It has been suggested (Dietz & Kendzior, 1994) that the minor mRNA species compete more effectively for primers when the full-length message is reduced in abundance.

A second model for the association of exon-skipping with nonsense mutation is "nuclear scanning," which has been used to explain exon-skipping in the human fibrillin gene (Dietz & Kendzior, 1994). It states that some unidentified nuclear process is able to recognize the presence of stop codons within exons (still separated by introns) and influence the selection of exons for splicing. This results in the nonsense-containing exon being omitted from the final, spliced mRNA. The nuclear scanning model has been tested by site-specific mutagenesis using transfected minigene constructs of the human fibrillin gene (Dietz & Kendzior, 1994). In this system, the altered splicing does not always eliminate a nonsense codon. Some structural effects of the nonsense mutations on splice-site selection are recognized (Dietz & Kendzior, 1994; Maquat, 1996). A clear connection between exon-skipping and "nonsense" is lacking for this gene: of eight nonsense mutations in the fibrillin gene that affect mRNA abundance, only one causes exon-skipping (Dietz & Pyeritz, 1995).

Neither the relative enrichment nor the nuclear scanning model have been verified experimentally in a conclusive manner for any gene (Maquat, 1995, 1996). The strong association between nonsense mutation and exon-skipping for the *hprt* gene of CHO cells and the availability of a large set of characterized mutants presented an opportunity for us to test the relative enrichment model for this gene.

RESULTS

Evaluation of missense and nonsense mutants for abundance of total mRNA and for the presence of exon-skipping

We used northern blot hybridization previously to determine the relative total *hprt* mRNA concentration in each of 84 CHO cell lines having mutations in the *hprt* gene (Newton et al., 1992a; Manjanatha et al., 1994). All 84 lines possessed different mutations; 35 were nonsense mutations and 49 missense mutations. We evaluated the same set of mutant cell lines for the presence of minor *hprt* mRNA species lacking one or more exons by an RT-PCR protocol (Newton et al., 1992a; Manjanatha et al., 1994), hereafter referred to as the preparative RT-PCR protocol because it was designed originally for preparing DNA sequencing templates for mutational analysis (see Materials and Methods). The exon-deleted species typically detected for nonsense mutants (deletion of exons 2, 2 and 3, and 2–4) are shown in Figure 1 (lane N). The only exception to missense mutants having a single product was mutant 237-1, which

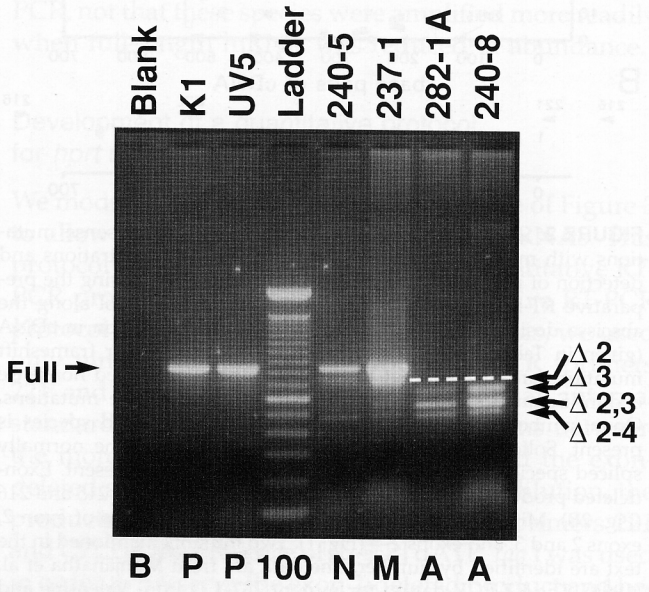

FIGURE 1. Agarose gel electrophoresis of *hprt* RT-PCR products from mRNA of various mutants and parental CHO lines (Valentine & Heflich, 1995). Messenger RNA was reverse transcribed and amplified with primers 215 and 216 (Fig. 2B) to amplify the entire *hprt* coding sequence by the preparative RT-PCR protocol (Newton et al., 1992a). The exon deletions found in each species by DNA sequencing are indicated at the side. B, blank, water for RNA; P, parental lines (K1, UV5); 100, 100-bp ladder; N, nonsense mutation in exon 2 (mutant 240-5); M, missense mutation in exon 2 (mutant 237-1); A, acceptor site mutations of exon 3 (mutants 282-1A, 240-8). Full, full-length (containing all exons), 838 bp; Δ2, deletion of exon 2, 731 bp; Δ3, deletion of exon 3, 654 bp; Δ2,3, deletions of exons 2 and 3, 547 bp; Δ2–4, deletion of exons 2–4, 481 bp.

had minor, exon-deleted products typical of nonsense mutants (Fig. 1, lanes M, N). One nonsense mutant (240-7), whose mutation in exon 5 is also a donor site mutation and which lacks exon 5 in the major RNA species, had only a single exon-deleted mRNA containing an exon 2–4 deletion (Valentine & Heflich, 1995). Exon-deleted mRNA species are not detected in RNA from the parental cell lines by the preparative protocol (Fig. 1, lanes P). A graphic representation of the data from these studies is presented in Figure 2A.

Two observations about nonsense mutations can be made from Figure 2A. First, all 19 of the nonsense mutants with multiple, minor mRNA species also have total mRNA levels below 20% of parental levels (18 were below 10%). These mutants include all those with nonsense mutations between the end of exon 2 and the beginning of exon 6. The 24 missense mutants with mutations in the same region are varied in their mRNA levels, but none is below 25% of parental levels. This variation in mRNA abundance may reflect the fact that each mutant line has gone through a selection process for the loss of *hprt* function, which may have affected mRNA levels. Second, with one exception, all mutants that display exon-skipping are nonsense mutants. The one missense mutant that displays exon-skipping (mutant 237-1) has a mutation in exon 2 at an adjacent nucleotide to a nonsense mutation (mutant 240-5; Table 1) that also is associated with exon-skipping. The nonsense mutant has *hprt* mRNA undetectable by northern blot, whereas the missense mutant has a normal abundance of *hprt* mRNA. Thus, even though this missense mutant was atypical in having exon-deleted products, it was typical of other missense mutants with regard to a normal abundance of total *hprt* mRNA.

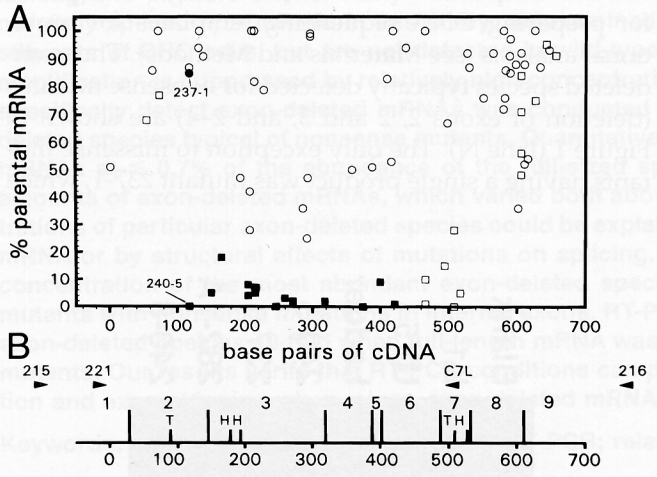

FIGURE 2. A: Scattergram comparing CHO *hprt* nonsense mutations with missense mutations for *hprt* mRNA concentrations and detection of minor, exon-deleted *hprt* mRNA species using the preparative RT-PCR protocol. The position of each symbol along the abscissa designates the position of a particular mutation in cDNA (given in Table 1 for selected mutations). Symbols for frameshift mutations are displayed at the position of the generated nonsense codon. Squares, nonsense mutations; circles, missense mutations. Open symbols indicate that only the normally spliced species is present. Solid symbols indicate that, in addition to the normally spliced species, exon-deleted minor species are also present. Exon-deleted products are detected by RT-PCR using primers 215 and 216 (Fig. 2B). Minor mRNAs include species with deletions of exon 2, exons 2 and 3, and exons 2–4 (Fig. 1). Two mutants mentioned in the text are identified by number. The data are from Manjanatha et al. (1994). The RT-PCR datum for mutant 237-1 is from Valentine and Heflich (1995) and the northern blot datum for 237-1 is from Newton et al. (1992a). This mutant was evaluated by northern blot in a semi-quantitative manner (high: 85–100%); a value of 85% was assigned arbitrarily. **B:** Exonic map of hamster *hprt* cDNA, aligned to scale of A. Tall vertical lines separate exons and numbers between lines indicate exon numbers. Numbering is from the first nucleotide of the initial AUG (Konecki et al., 1982). Positions of PCR primers are indicated by arrowheads. Positions of restriction enzyme sites are shown by short vertical bars; *Taq* I restriction sites are indicated by T, *Hae* III sites by H. The size of each exon that contributes to coding sequence is exon 1, 27 bp; exon 2, 107 bp; exon 3, 184 bp; exon 4, 66 bp; exon 5, 18 bp; exon 6, 83 bp; exon 7, 33 bp; exon 8, 77 bp; exon 9, 48 bp.

Detection and sequencing of exon-deleted cDNAs from parental lines

The detection of exon-deleted mRNAs from one missense mutant (237-1) prompted us to consider the possibility that these exon-deleted *hprt* mRNA species were present in the parental cell lines (even though their amplification products were not visible in Fig. 1, lanes P). Exon-deleted mRNAs may have been enriched to the point of detection in the nonsense mutants because of the reduction in the amount of the normally spliced mRNA. This is basically the relative enrichment model. We hypothesized tentatively that the missense mutation in 237-1 has a structural effect on splicing that increases concentrations of exon-deleted species in the cell.

In order to test whether or not *hprt* mRNAs with exon deletions were present in the parental cell lines, we reamplified RT-PCR products after the full-length product had been digested by a restriction enzyme (Belgrader & Maquat, 1994). The *hprt* mRNA was first amplified by our preparative protocol using primers 221 and 216 (Fig. 2B). Primer 221 was used in order to include a control with cloned *hprt* cDNA as the template (the cloned cDNA does not include the sequence for primer 215). The purified products of this reaction were digested with either *Taq* I or *Hae* III, which cut within the deleted exons (Fig. 2B). The digests were diluted and reamplified with primer 221 and a nested primer complementary to sequence in exon 7 (C7L, Fig. 2B). More than 90% of the full-length *hprt* cDNA was cleaved during *Taq* I digestion (Fig. 6A) and *Hae* III digestion was found to be even more efficient (Fig. 3A). Either enzyme permitted detection of multiple exon deletions involving both exons 2 and 3; *Taq* I allowed detection of the deletion of exon 2 only and *Hae* III allowed detection of the deletion of exon 3 only.

The products of the reamplification reactions for parental cell lines and selected mutants (used as positive

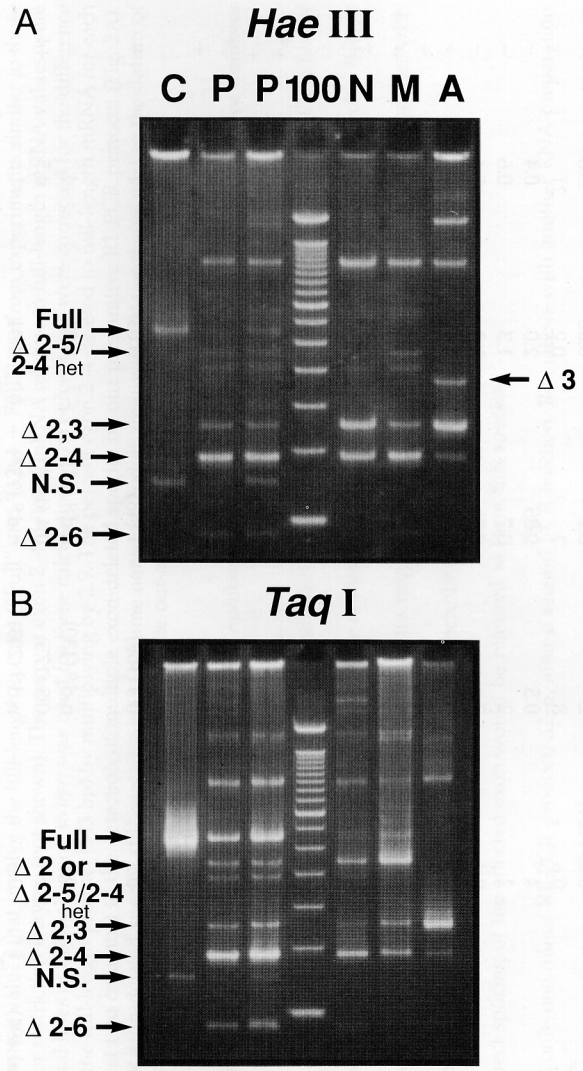

FIGURE 3. Reamplification of *hprt* RT-PCR products with primers 221 and C7L after digestion with restriction enzymes. Products were separated on an acrylamide gel and stained with ethidium bromide. Identities determined for the exon-deleted species (by DNA sequencing) are indicated at the side. C, cloned Chinese hamster *hprt* cDNA; P, parental CHO lines K1 (lane 2) and UV5 (lane 3); 100, 100-bp ladder; N, nonsense mutation in exon 2 (mutant 240-5); M, missense mutation in exon 2 (mutant 237-1); A, acceptor site mutation of exon 3 (mutant 240-8). N.S. stands for a "nonspecific" product due to priming of the C7L primer at position 97. **A:** *Hae* III digestion. "Δ2–5/2–4 het" was sequenced only for P lanes. Full-length, 543 bp; Δ2, 436 bp; Δ3, 359 bp; Δ2,3, 252 bp; Δ2–4, 186 bp; Δ2–6, 85 bp; N.S., 145 bp; Δ2–5/2–4 het, heteroduplex of Δ2–5 and Δ2–4. The Δ2–5 sequence is 168 bases long, but was found only in a heteroduplex band with Δ2–4 and migrated at 436 bp. **B:** *Taq* I-digestion. The Δ3 band is destroyed by *Taq* I. The band at 436 bp in lanes 2, 5, and 6 contained only an exon 2 deletion, but in lane 3 contained primarily the heteroduplex of Δ2–5/Δ2–4 and probably also Δ2. The band just below the heteroduplex band (~390 bp) contained a sequence the same as an exon 2–4 deletion (about twice the expected size, possibly a dimer aggregate).

controls for exon-deleted species) were separated on acrylamide gels (Fig. 3), eluted from the gels, and sequenced. RNA from the two parental lines, K1 and UV5, produced amplification products with deletions of exons 2, 2 and 3, 2–4, 2–5, and 2–6 (Fig. 3). The 2–5-deleted species was not found at its expected size (168 bp), but as part of a heteroduplex with the exon 2–4-deleted product. This heteroduplex migrated at the same position as the exon 2-deleted product (436 bp). Digestion with *Hae* III (Fig. 3A) removed the exon 2-deleted product and allowed sequencing of the heteroduplex. All of the exon-deleted species involving exons 2 and 3 that were found in mRNA from our mutant collection (Valentine & Heflich, 1995) were detected in the parental lines, with the exception of a singly deleted exon 3 species. The deletion of exon 3 alone was found only for mutants with acceptor site mutations of exon 3 (Fig. 1, lanes A; Fig. 3A, lane A). Significantly, none of these exon-deleted products were detected in the amplification of cloned *hprt* cDNA (Fig. 3, lanes C), indicating that they reflected mRNA species specific to CHO cells and were not artifacts of PCR amplification.

Quantitative RT-PCR of exon-deleted mRNAs

Having demonstrated that the exon-deleted *hprt* mRNAs were present in the parental cell lines, it was necessary to quantitate their levels to see if nonsense mutation was associated with an elevated amount of exon-deleted species. If so, it could be argued that nonsense mutation increased the abundance of exon-deleted mRNAs to a point that was detectable by RT-PCR, not that these species were amplified more readily when full-length mRNA was reduced in abundance.

Development of a quantitative protocol for *hprt* mRNAs

We modified the reamplification procedure of Figure 3 to allow a quantitative analysis of *hprt* mRNAs. This protocol is hereafter referred to as the quantitative RT-PCR protocol, as opposed to the preparative RT-PCR protocol (Figs. 1, 2). For quantitative analysis, we used only nine cycles for the first round of PCR (primers 221 and 216, as well as *aprt* primers for an internal standard) in order to minimize interactions between the more abundant full-length species and the exon-deleted species. After *Taq* I digestion and dilution, the products were reamplified for 26 cycles (primers 221 and C7L) in the presence of [α-^{32}P] dATP. *Taq* I was used in order to preserve the exon 2-deleted product and because *Hae* III digestion destroyed the *aprt* standard.

The quantitative character of the protocol was evaluated by analyzing twofold serial dilutions of total RNA from the parental line K1. Analyses of the *aprt* standard, full-length species, and exon-deleted products are shown in Figure 4. The amount of RNA used in our preparative protocol, 1 μg/100 μL PCR reaction mix (Newton et al., 1992a), was beyond the linear range of amplification for the *aprt* standard (Fig. 4A) and the full-length *hprt* species (Fig. 4B). The exon-deleted

TABLE 1. Relative concentrations of exon-deleted and full-length *hprt* mRNAs by quantitative RT-PCR.[a]

Cell line/mutant#[c] (Parental line)	Mutation				mRNA Species					
					Relative to parental cell line[b]				Same mutant/line	
	Position[d]	Sequence change	Exon[e]	Type[f]	Δ2[g]	Δ2,3[g]	Δ2-4[g]	Full[h]	Δ2-4 ÷ Full × 100 (%)	Multiple products[i]
K1	—	—	—	—	1.0	1.0	1.0	1.0	0.4	−
UV5	—	—	—	—	1.0	1.0	1.0	1.0	0.7	−
240-5 (K1)	118	G → T	2	non	6	4	2	0.03	17	+
237-1 (K1)	119	G → T	2	mis	28	11	3	0.5	2	+
264-0 (K1)	54-I2:+16	deletion	2	del (Δ2; in)	2,100	635	15	1.8[j]	4	+
Exon 2/3 boundary 134/135										
282-1A (UV5)	I2:-2	A → T	3	acc (Δ3; out)	n.d.[k]	60	2	0	—[l]	+
240-8 (K1)	I2:-1	G → T	3	acc (Δ3; out)	n.d.[k]	230	13	0	—[l]	+
71-2 (K1)	139	G → T	3	non	0.05 (109)	2	0.2	0.02	5.0	+[m]
282-2B (UV5) (NS3F)	205	A → T	3	non	0.6	8	2	0.2	21	+
240-4 (K1) (MS3G)	211	G → T	3	mis	4	0.5	0.85	2.0	0.4	−
282-8C (UV5) (MS3I)	215	A → C	3	mis	2	2	0.7	1.3	0.6	−
81-3 (K1) (MS3J)	229	G → T	3	mis	0.4	7	0.8	1.3	0.4	−
238-1 (K1) (NS3I)	232/233	+T	3	non (ochre at 246)	0.25	2	0.9	0.004	64	+
282-5C (UV5) (NS3J)	259	A → T	3	non	1.5	4	2	0.09	22	+
282-9C (UV5) (NS3K)	271	A → T	3	non	1.9	0.3	0.7	0.02	25	+
235-0 (K1) (MS3L)	292	G → T	3	mis	0.1	0.4	0.4	0.25	0.3	−
284-5C (K1) (MS3N)	297	T → A	3	mis	0.3	0.3	0.9	0.3	0.6	−
Exon 3/4 boundary 318/319										
233-0-2UA (UV5)	329	C → T	4 (Δ4; in)	mis	n.d.[k]	n.d.[k]	9	1[n]	3	+[o]
251-7 (UV5)	329	C → G	4 (Δ4; in)	non	n.d.[k]	n.d.[k]	3	0.3[n]	6	+[o]
282-3C (UV5)	333–336	−G	4 (Δ4; in)	non (ochre 339)	n.d.[k]	n.d.[k]	5.5	0.15[n]	19	+[o]
282-8A (UV5) (NS4A)	374	T → A	4	non	0.4	1.6 (73)	2	0.004	190	+
Exon 4/5 boundary 384/385										
240-7 (K1)	400	G → T	5 (Δ5; in)	non; don	0.2	0.3 (109)	1 (43)	0.03[p]	4	+
Exon 5/6 boundary 402/403										
282-4B (UV5) (NS6A)	421	A → T	6	non	0.3	n.d.[q] (130)	n.d.[q] (64)	0.02	4	+
282-6B (UV5) (NS6D)	466	A → T	6	non	1	0.8 (175)	0.4 (109)	0.1	4.5	+[r]
240-9 (K1) (NS6B)	465	−C	6	non (opal 494)	0.6	n.d.[q] (203)	n.d.[q] (137)	0.04	1	−

[a]Mutants are listed in the order of the nonsense codons in the *hprt* gene. The quantitative values for exon-deleted species are from the panels of Figure 5, which have been compared to the appropriate parental cell line after normalization to the *aprt* standard. Quantitative values that involve the full-length species ("Full" and "Δ2–4 ÷ Full") are from experiments similar to those in Figure 5, but in which a mock digestion was done with water substituted for restriction enzyme (not shown). The percent exon 2–4-deleted mRNA relative to full-length mRNA values were calculated from the mock digestions for each mutant; no comparison to parental lines or normalization to *aprt* was used for these calculations. The percentages were corrected for the difference in size in base pairs between the exon 2–4-deleted PCR product (186 bp) and the full-length product (543 bp) by multiplying by 2.9. The percent exon 2–4-deleted to full-length mRNA for each mutant determined by the quantitative RT-PCR protocol is also compared (last two columns) to the detection of multiple exon-deleted species by our preparative RT-PCR protocol (Fig. 2A). The number of bases between the initiating AUG and the nonsense codon for exon-deleted species still containing an in-frame nonsense codon are given in parentheses next to the datum of the appropriate species. The exon 2-deleted species is not included because all have nonsense at base 33, resulting from the out-of-frame exon 2 deletion.

[b]n.d., species not discernable.

[c]MS, NS designations are alternate names for same mutant from Manjanatha et al. (1994).

[d]Position of mutation in cDNA (numbering from the initiating AUG; Konecki et al., 1982). "I" indicates intron, positive numbers start at the 5′ end (next to donor site); negative numbers go backward from the 3′ end (acceptor site).

[e]Exon that contains mutation.

[f]non, nonsense; mis, missense; del, deletion; acc, acceptor site; don, donor site. If the major mRNA species contains an exon deletion, the exon deletion is designated by Δ and the effect of the deletion on the reading frame is indicated ("in," in-frame; "out," out-of-frame).

[g]Numbers in parentheses indicate the number of bases between the first base of the initiating AUG and the first base of the nonsense codon still contained in the exon-deleted species. Except for mutant 71-2, all exon 2 deletions terminate after 33 bases because exon 2 deletions are out-of-frame.

[h]For mutants where the major species has an exon deletion (from inactivation of a consensus splice site or an exonic site affecting splicing), the full-length species is taken as the species with the single, skipped exon, indicated in a footnote.

[i]Identified by the preparative RT-PCR protocol (Fig. 2A; Newton et al., 1992a; Manjanatha et al., 1994; Valentine & Heflich, 1995).

[j]Exon 2 is deleted.

[k]No species is expected here because the major species lacks an exon; correct splicing of the affected exon would be required to form this species.

[l]No full-length species present.

[m]We reported previously (Valentine & Heflich, 1995) that this mutant had only one minor RT-PCR product, Δ2–6, after a second PCR reaction. Reanalysis with another RNA preparation showed that this mutant had the products typical of other nonsense mutants.

[n]Exon 4 is deleted.

[o]The presence of multiple RT-PCR products was not reported in Valentine and Heflich (1995) by oversight; however, the exon 2–4 deletion product was clearly visible in addition to the deletion of exon 4. Mutant 233-0-2UA also showed a product of an appropriate size for an exon 2 and 4 deletion.

[p]Exon 5 is deleted.

[q]RT-PCR products are detected when four times greater input RNA is used; these species still contain in-frame nonsense codons.

[r]Although reported negative in Manjanatha et al. (1994) and consequently in Figure 2A (base 466), an exon 2–4-deleted species was detected on reanalysis. The original scoring reflects some subjective judgement; this mutant could have been reported as having two mRNAs, as for mutant 240-7.

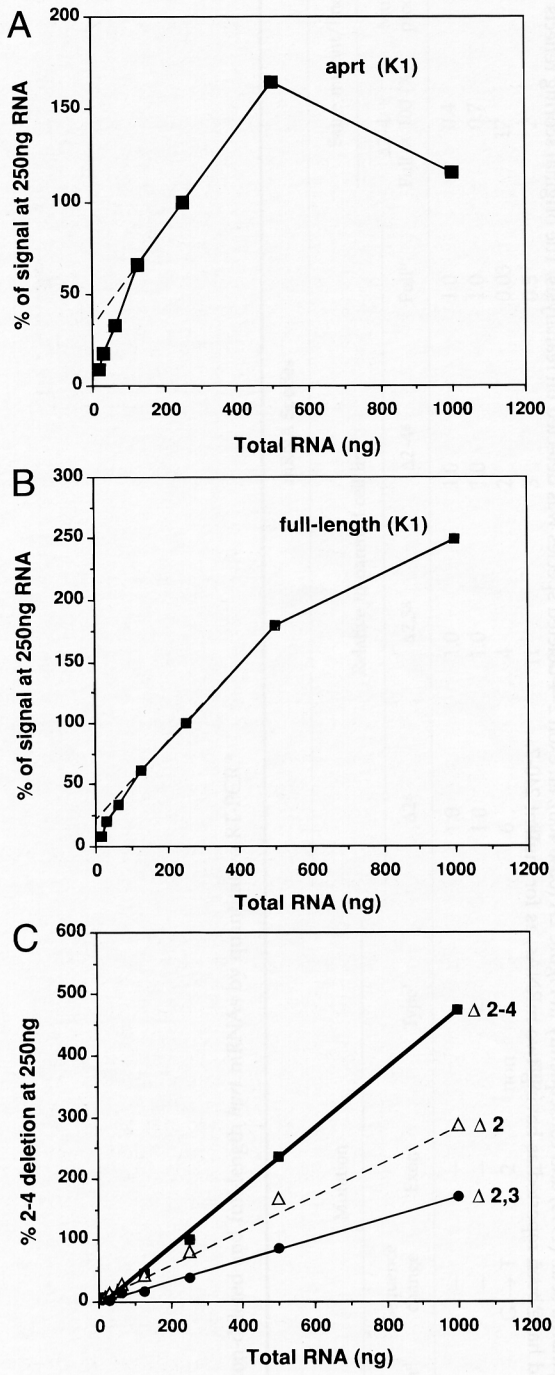

FIGURE 4. Relative concentration of *hprt* RT-PCR products amplified by the quantitative RT-PCR protocol as a function of amount of input RNA. *Taq* I digestion followed nine cycles of RT-PCR; after dilution, the products were reamplified for 26 cycles (primers 221 and C7L) in the presence of [α-^{32}P]dATP. Quantitative analyses are expressed as a percentage of the signal obtained using 250 ng input RNA, which was the amount chosen for further quantitative experiments. **A:** Amplified *aprt* cDNA standard from the parental line K1 (77 bp). **B:** Amplified full-length cDNA species (normally spliced) of parental line K1 (543 bp). **C:** Amplified cDNA of the three exon-deleted species: Δ2, deletion of exon 2 (436 bp); Δ2,3, deletion of exons 2 and 3 (252 bp); Δ2–4, deletion of exons 2–4 (186 bp). No correction was made for the difference in molecular weight between the different exon-deleted species.

mRNAs were in their linear amplification range throughout the dilution series (Fig. 4C) and were linear well above these concentrations as determined by a similar experiment with the deletion mutant 264-0, which overproduced these species (not shown). The most abundant exon-deleted mRNA species had the deletion of exons 2–4 (Fig. 4C). When corrected for the difference in size, the 2–4-deleted species was four times more abundant than the exon 2-deleted species.

Subsequent experiments were conducted with 250 ng of total RNA/100 μL PCR reaction in order to have all species in a linear range of amplification. For comparison between cell lines, the quantitative results were normalized to the *aprt* product, with corrections for the dual linearity of the *aprt* standard curve. We considered that results from this assay were accurate within a factor of two.

Analyses of RNA from parental and mutant cell lines

The quantitative RT-PCR protocol was used to determine the concentrations of the various *hprt* mRNA species in both parental cell lines, in a set of mutant cell lines selected from those analyzed in Figure 2A, and in a group of additional mutants (264-0, 240-8, 282-1A, 233-0-2UA, 251-7, and 282-3C) that had single exon deletions in the major *hprt* mRNA species and that were selected for comparative purposes.

Comparison of the *hprt* mRNA products amplified by the quantitative RT-PCR protocol from mutants with mutations in exon 2 is shown in Figure 5A. The parental line for all mutants in this panel is shown in the first lane marked "P." For the nonsense mutant (lane N), levels of the three exon-deleted *hprt* mRNAs were elevated from two- to sixfold over parental concentrations (Table 1, mutant 240-5). The missense mutant (lane M), whose mutation was adjacent to that of the nonsense mutant, had amounts that were 3- to 30-fold greater than parental (Table 1, mutant 237-1). For the deletion mutant (lane D), which had no exon 2 donor site, increases of the exon-deleted mRNA were from 15- to 2,000-fold (Table 1, mutant 264-0). For all three of these mutants, the exon 2-deleted species was the most greatly increased. The abundance of the major mRNA species in the nonsense mutant was reduced to 3% of the parent, but was relatively normal in the missense and deletion mutant (Table 1; the full-length species is not quantitative in Figure 5 because *Taq* I digestion has reduced its concentration). Although the nonsense mutant had some increase in the abundance of exon-deleted species, we confirmed our expectation that the missense mutant contained a substantial increase in the abundance of exon-deleted species.

Figures 5B–E show the same comparison for CHO mutant cell lines containing nonsense (N) and mis-

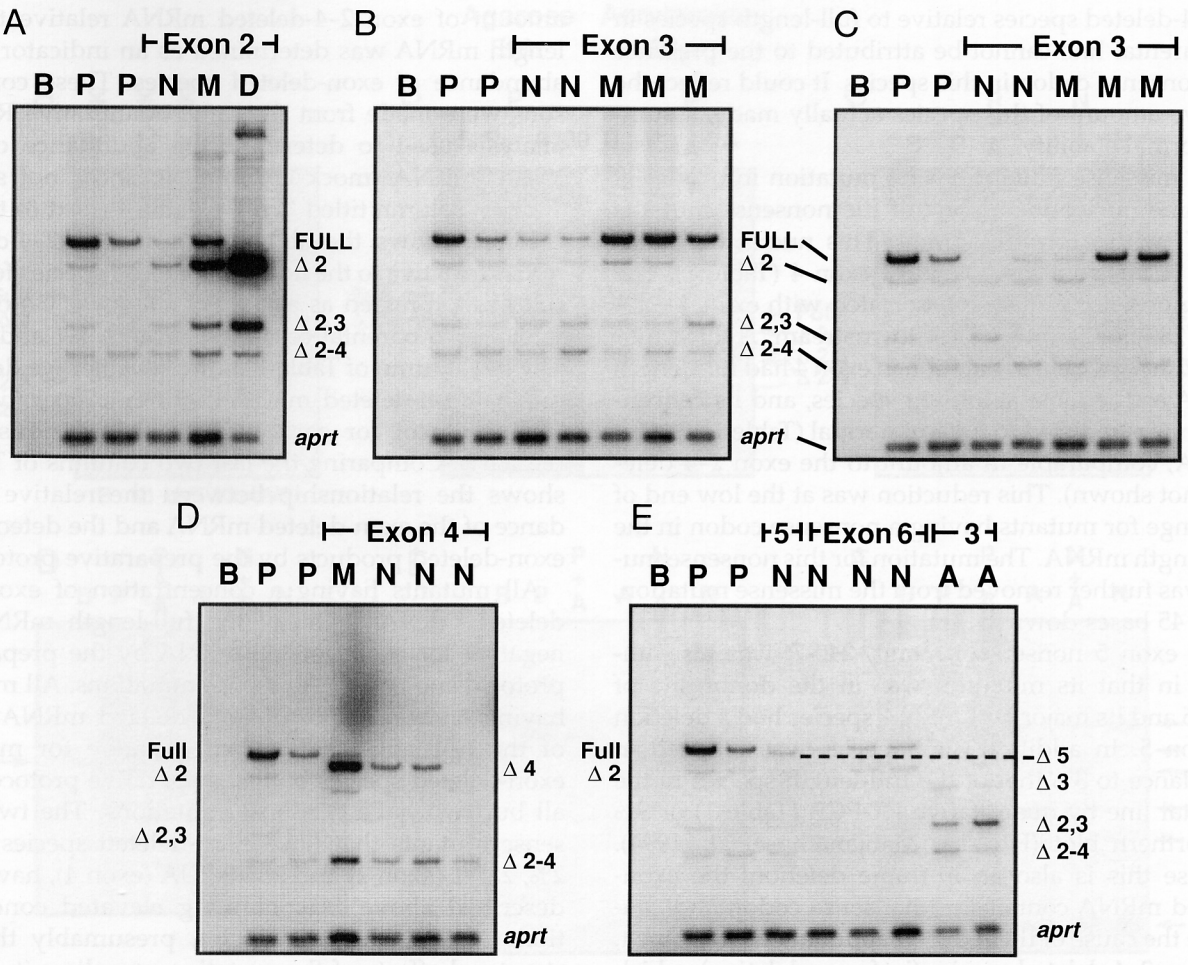

FIGURE 5. Acrylamide-gel separations of radioactive PCR products from quantitative RT-PCR (primers 221 and C7L) of *hprt* mutants. B, blank; P, parental lines K1 (lane 2) and UV5 (lane 3) in each panel; N, nonsense mutant; M, missense mutant; D, deletion mutant; A, acceptor site mutant. Full-length and exon 3-deleted species are not quantitative because they have been reduced by *Taq* I digestion. Quantitative comparisons between mutants and parent strains for each exon-deleted species are shown in Table 1. Information giving parental line of each mutant, exon-containing mutation, and cDNA position of nonsense codons is also given in Table 1. Mutants are in order from left to right through panels A–E as the mutations they contain are distant from the 5′ end of the gene. Identities of mutants for each panel are as follows. **A:** Lanes 4–6: 240-5, 237-1, 264-0. **B:** Lanes 4–8: 71-2, 282-2B, 240-4, 282-8C, 81-3. **C:** Lanes 4–8: 238-1, 282-5C, 282-9C, 235-0, 284-5C. **D:** Lanes 4–7: 233-02UA, 251-7, 282-3C, 282-8A. **E:** Lanes 4–9: 240-7, 282-4B, 240-9, 282-6B, 282-1A, 240-8. Lanes E6 and E7 should be reversed to match the order in Table 1 and Figure 2A, which are in the order of the nonsense codons from the 5′ end of the gene (rather than the order of the mutations). Numbers above the lettering are exon numbers. The exon 5-deleted species is 525 bp. Sizes of other fragments are the same as in Figure 3.

sense (M) mutations throughout exons 3–6 as well as two acceptor site (A) mutations of exon 3. There was no general increase of exon-deleted *hprt* mRNAs for nonsense mutants compared to missense mutants (Table 1). However, as for mutants with mutations in exon 2, several of these mutants had concentrations of individual exon deleted mRNAs that differed from those in parental cells.

Three mutants with mutations in exon 4 were unusual in that they lacked exon 4 in the major mRNA species and they had an increased abundance of exon 2–4-deleted mRNA; one was a missense mutant and two were nonsense mutants (Fig. 5D, lane M, first two lanes marked "N;" Table 1, mutants 233-0-2UA, 251-7, and 282-3C). The missense mutant had the greatest increase in the exon 2–4-deleted mRNA, ninefold. Also, no exon 2-deleted or exon 2 and 3-deleted species was found in any of these mutants, suggesting that little correct splicing of exon 4 took place because of the mutations. These species may have been shifted to the exon 2–4-deleted mRNA, because it was increased, or to a unique band, which was an appropriate size to contain an exon 2 and exon 4 deletion (Fig. 5D, lane M).

The missense mutant had a normal abundance of the exon 4-deleted mRNA relative to parental full-length mRNA, whereas these two nonsense mutants had somewhat reduced amounts, 30% for mutant 251-7 and 15% for mutant 282-3C (Table 1). Exon 4 deletions are in-frame, so these reductions in abundance of the

exon 4-deleted species relative to full-length species in the parental line cannot be attributed to the presence of a nonsense codon in this species. It could reflect the relative amount of this species actually made, assuming normal stability.

The missense mutant has its mutation in exon 4 at the same nucleotide as one of the nonsense mutants (251-7) with exon 4 skipping. This nucleotide is located 11 bp from the 5′ end of exon 4 (Table 1). The other nonsense mutation associated with exon 4 skipping (282-3C) is four bases downstream. A third mutant with a nonsense mutation in exon 4 had full-length mRNA as the most abundant species, and its concentration was reduced to 0.4% of normal (Table 1, mutant 282-8A; comparable in amount to the exon 2–4 deletion, not shown). This reduction was at the low end of the range for mutants having a nonsense codon in the full-length mRNA. The mutation for this nonsense mutant was further removed from the missense mutation, being 45 bases downstream.

The exon 5 nonsense mutant, 240-7, was also unusual in that its mutation was in the donor site of exon 5 and its major *hprt* mRNA species had a deletion of exon 5. In addition, this species was reduced in abundance to 3% that of the full-length species in the parental line by quantitative RT-PCR (Table 1) or 9% by northern blot (Fig. 2A; Manjanatha et al., 1994). Because this is also an in-frame deletion, the exon-deleted mRNA contains no nonsense codon and cannot be the cause of the reduced abundance. In contrast, the exon 2–4-deleted species (in-frame deletion), which still retains exon 5 and the nonsense codon (Valentine & Heflich, 1995), showed no reduction in relative abundance (Table 1). Faint bands below each exon-deleted species may represent additional deletions of exon 5 (Fig. 5E, N in exon 5).

Two mutants with mutations in the acceptor site of exon 3, included for comparison, had a 2- to 200-fold increase in the relative abundance of exon-deleted mRNAs (Fig. 5E, lanes A; Table 1, 282-1A and 240-8). There was no quantifiable full-length product in mutant 240-8 (Fig. 6B,C,D, lanes A). In contrast, the deletion mutant with no exon 2 donor site caused no reduction in abundance of the major, exon 2-deleted species (Fig. 6A, lane D; Table 1, increased 1.8-fold, mutant 264-0). Missense mutant 233-0-2UA also had a normal abundance of exon 4-deleted mRNA (Fig. 6D, lane M; Table 1).

Abundance of exon 2–4-deleted mRNA relative to full-length mRNA in mutant and parental cells

We demonstrated above that the exon 2–4-deleted product was the most abundant exon-deleted product for the parental line K1 (Fig. 4C). Figure 5A (lanes P) shows that the exon 2–4-deleted species is even more predominant for the parental line UV5. Therefore, the amount of exon 2–4-deleted mRNA relative to full-length mRNA was determined as an indicator of the abundance of exon-deleted species. These comparisons were made from the same quantitative RT-PCR analysis used to determine the abundance of full-length mRNA (mock enzyme digestion, not shown; Table 1, column titled "Full"). Table 1 (next to the last column) shows the abundance of exon 2–4-deleted mRNA relative to the normally spliced species for each cell line expressed as a percent. This was 0.4 or 0.7% for the two parental cell lines (Table 1, K1 and UV5). The last column of Table 1 shows whether we detected minor, exon-deleted mRNAs by our preparative RT-PCR protocol for each cell line in previous work (Fig. 2A). Comparing the last two columns of Table 1 shows the relationship between the relative abundance of the exon-deleted mRNA and the detection of exon-deleted products by the preparative protocol.

All mutants having a concentration of exon 2–4-deleted mRNA $< 2\%$ of the full-length mRNA are negative for exon-deleted mRNA by the preparative protocol and contain missense mutations. All mutants having an abundance of exon-deleted mRNA $\geq 2\%$ of the full-length mRNA are positive for multiple exon-deleted species by the preparative protocol, and all but two have nonsense mutations. The two missense mutants that have exon-deleted species above 2%, 237-1 (exon 2) and 233-0-2UA (exon 4), have been described above as containing elevated concentrations of exon-deleted species, presumably through structural effects of the mutation on splice site recognition (see Discussion).

Suppression of the amplification of minor, exon-deleted mRNA by the preparative protocol

We had designed our quantitative RT-PCR protocol to reduce the amount of full-length product by restriction enzyme digestion so it would not inhibit the amplification of the minor products. The quantitative nature of the protocol is demonstrated in Figure 4. However, a direct comparison of enzyme digestion to mock digestion using this protocol showed that the level of the exon 2–4-deleted species was the same with and without enzyme digestion (Fig. 6A; Table 2A). This indicated that abundant full-length species did not suppress the amplification of exon-deleted cDNA under the conditions of the quantitative protocol.

We therefore determined whether there was an inhibitory effect on the amplification of exon-deleted products when amplified by the preparative RT-PCR protocol used to generate the data in Figure 2A. We mixed RNA from our parental cell line K1 with RNA from mutant 240-8, which had a mutation in the acceptor site of exon 3 and contained abundant exon-deleted *hprt* mRNA, but no full-length species (Fig. 2,

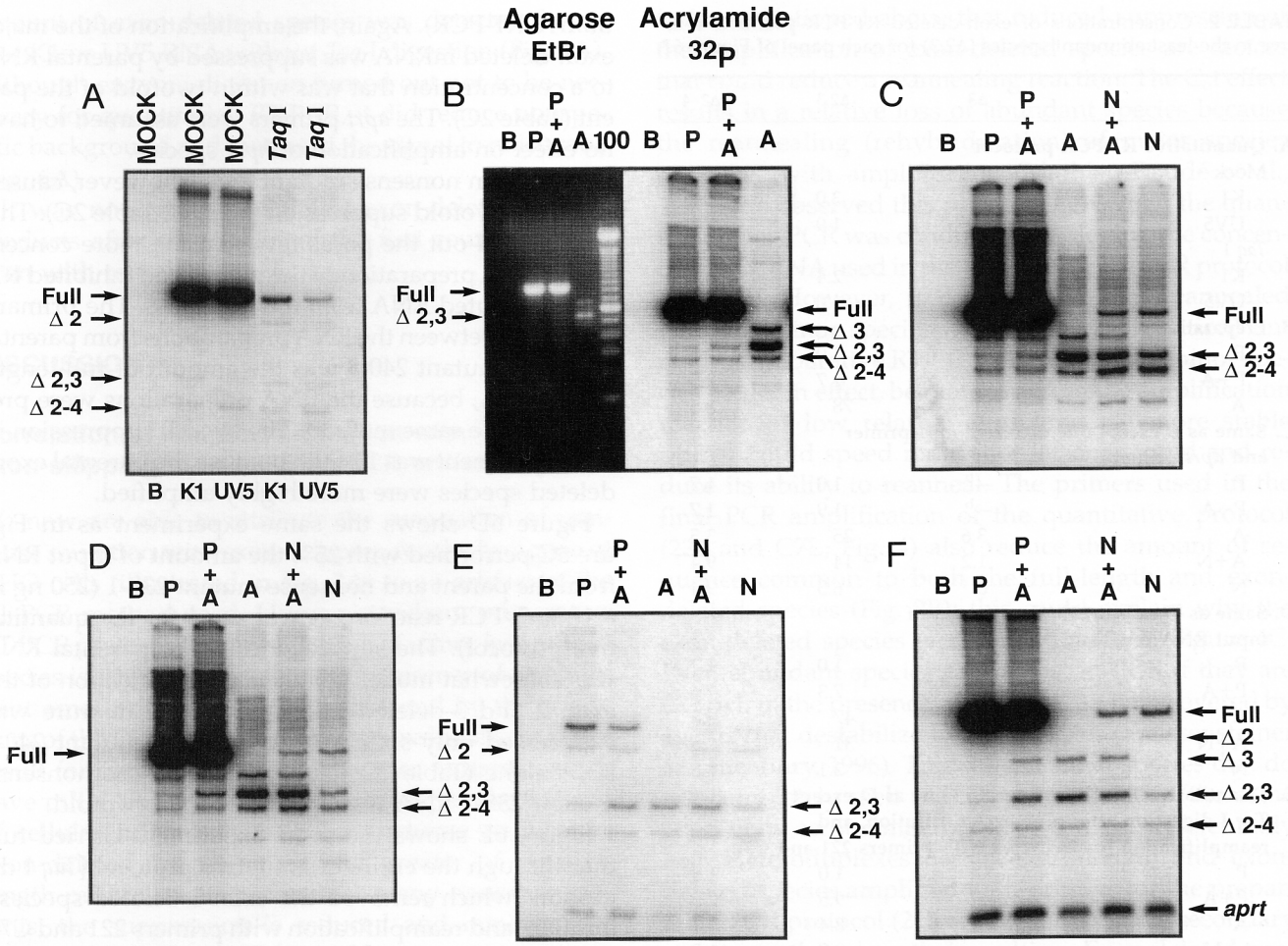

FIGURE 6. Effects of PCR conditions that differ between the preparative RT-PCR protocol and the quantitative RT-PCR protocol on the amount of exon-deleted *hprt* cDNA products obtained. Quantitative data from this figure appear in Table 2. B, blank; P, parental line, K1; N, nonsense mutant 238-1; A, acceptor site mutant 240-8. Mixtures are indicated by +. Except for panel B, all reactions contained *aprt* primers even though the *aprt* product is not included in all reproductions. **A:** Quantitative RT-PCR. Quantitative comparison of exon-deleted products formed with and without enzyme digestion. The mock samples had water added for enzyme. Mock and *Taq* I lanes were on the same gel, but four lanes between them have been removed electronically. **B:** Preparative RT-PCR. Amplification of *hprt* gene using preparative protocol (1 μg RNA, primers 215 and 216, 30 cycles of PCR) except that α-[^{32}P]dATP was added in the same quantity as for quantitative PCR and the RNA from the acceptor site mutant 240-8 was diluted 10-fold. The left half of panel A shows an ethidium bromide-stained agarose gel as done for the preparative protocol and the right half shows the same samples on an acrylamide gel scanned for radioactivity. **C:** Same PCR conditions as for B, except substituting primer 221 for 215 and adding *aprt* primers. **D:** Same conditions as for C, except input RNA for samples P and N was 25% of that in C. **E:** Quantitative RT-PCR protocol. Same as D, except samples were stopped after nine cycles, digested with *Taq* I, and reamplified with primers 221 and C7L and [^{32}P]dATP for 26 cycles. **F:** The same samples as in panel E were amplified similarly by the quantitative protocol, except that a mock restriction enzyme digestion substituted water for enzyme.

second lane marked "A"). Because mutant 240-8 had exon-deleted mRNA concentrations that were 10–100 times greater than the parent (Table 1), its RNA was diluted 10-fold before mixing. RT-PCR was conducted by the preparative protocol, but [α-^{32}P]dATP was included in the PCR reaction, as for quantitative RT-PCR, in order to identify and quantify the minor products formed by the parental line.

Figure 6B shows the effect of adding parental RNA to RNA from the mutant both by ethidium bromide staining on an agarose gel and by phosphorimaging of an acrylamide gel. Parental RNA suppressed dramatically (more than 40-fold, Table 2B) the amplification of the major exon-deleted *hprt* mRNA of the mutant (deletion of exons 2 and 3). This was within twofold of the level of the same exon-deleted species amplified from parental RNA itself. Although minor products were not seen for the parental cell line by ethidium bromide staining on the agarose gel, they were detected with radiolabeling on an acrylamide gel. This experiment demonstrated that RNA from parental cells did inhibit the amplification of exon-deleted species, but it did not specifically address the question of whether the abundant full-length mRNA was responsible for this suppression.

Several differences between our preparative procedure and the quantitative RT-PCR protocol existed, and we proceeded to test these variables systemati-

TABLE 2. Concentrations of exon-deleted RT-PCR products relative to the least abundant species (Δ2,3) for each panel of Figure 6.[a]

	Δ3	Δ2,3	Δ2–4
A. Quantitative RT-PCR protocol			
Mock			
K1	—	3.0	4.2
UV5	—	1.9	7.9
Taq I			
K1	—	2.4	5.3
UV5	—	1.0	8.1
B. Preparative RT-PCR protocol			
P	—[b]	1.0	2.5
P+A	1.2	1.7	2.5
A	20	78	8.5
C. Same as B except one different *hprt* primer and *aprt* primers			
P	—[b]	1.0	1.7
P+A	—[b]	1.9	1.7
A	3.6	25	3.5
A+N	1.2	14	9.4
N	0	6.5	9.4
D. Same as C except 25% the amount of input RNA for P and N			
P	—[b]	1.0	1.2
P+A	—[b]	7.3	1.4
A	7.3	47	6.8
A+N	3.9	31	7.9
N	0	2.1	2.5
E. Quantitative RT-PCR protocol: Same as D except *Taq* I digestion after nine cycles, dilution, and reamplification for 26 cycles with primers 221 and C7L			
P	—	1.0	1.9
P+A	—	9.5	2.5
A	—	8.4	1.4
A+N	—	9.7	1.9
N	—	1.4	1.2
F. Same as E except mock enzyme digestion (water for *Taq* I)			
P	—	1.0	1.6
P+A	—	10	2.6
A	—	18	2.0
A+N	—	12	2.0
N	—	2.2	1.5

[a]Row designations are the same as the lane headings of Figure 6; column headings are the same as the labels in Figure 6.

[b]This band from the parent (P) is the result of nonspecific amplification because it disappeared after *Hae* III digestion (Fig. 3A).

cally in order to identify which was responsible for the suppressive effect on the amplification of exon-deleted species. We also used RNA from mutant 238-1, which had a frameshift mutation causing nonsense and contained a greatly reduced concentration of full-length *hprt* mRNA (Table 1), for mixing with RNA from mutant 240-8 in order to determine the contribution of abundant full-length mRNA to suppression. Figure 6C shows the results of mixing diluted RNA from acceptor site mutant 240-8 with either the parental RNA or RNA from the nonsense mutant 238-1 and amplification using primer 221 instead of 215 and *aprt* primers (i.e., the primers used for the first round of the quantitative RT-PCR). Again, the amplification of the major exon-deleted mRNA was suppressed by parental RNA to a concentration that was within twofold of the parent (Table 2C). The *aprt* primers were assumed to have no effect on amplification of *hprt* species.

RNA from nonsense mutant 238-1, however, caused less than twofold suppression (Fig. 6C; Table 2C). This result ruled out the possibility that the more concentrated RNA preparation of the parent had inhibited RT-PCR of diluted RNA from mutant 240-8. The primary difference between the RNA preparations from parental cells and mutant 240-8 was the amount of full-length *hprt* mRNA, because the RNA preparations were prepared by the same method. The overall suppression in this experiment was 13-fold, because the parental exon-deleted species were more highly amplified.

Figure 6D shows the same experiment as in Figure 6C performed with 25% the amount of input RNA from the parent and nonsense mutant 238-1 (250 ng in a 100-μL PCR reaction, as was used for the quantitative protocol). The suppression by the parental RNA was somewhat moderated in that amplification of the exon 2 and 3-deleted mRNA from the mixture was suppressed only sixfold relative to the mutant 240-8 RNA alone (Table 2D); suppression by the nonsense mutant 238-1 RNA was again less than twofold.

Figure 6E shows the same experiment carried further through the entire quantitative protocol [*Taq* I digestion (which removed the exon 3-deleted species), dilution, and reamplification with primers 221 and C7L and *aprt* primers for 26 cycles instead of 30]. No suppression was seen by either parent or nonsense mutant RNA; the amount of product from mixtures was instead additive. There are several differences between panels D and E: a 333-fold dilution accompanying enzyme digestion, reamplification with four fewer cycles of PCR, and the use of a nested lower primer, C7L. The dilution effectively reversed the amplification of the first nine cycles because $2^9 = 512$. We performed the same mixing experiment by the preparative protocol with only 26 cycles and found a 10-fold suppression (not shown) compared to 40-fold with 30 cycles. Therefore, the shorter cycle number may have been the major factor in eliminating the sixfold suppression that occurred in the absence of abundant full-sized mRNA and reduced RNA input (Table 2D). The remaining twofold difference may be attributed either to the dilution or the different lower primer.

Figure 6F shows a mixing experiment identical to Figure 6E (quantitative protocol) except that the same samples were carried through a mock enzyme digestion (water for *Taq* I). Amplification of exon 2 and 3-deleted mRNA was suppressed less than twofold by the addition of RNA from either parental cells or nonsense mutant 238-1 (Table 2F). This minor difference seems to be related more to mixing RNA samples than from enzyme digestion because no decrease in the

amount of exon-deleted species was detected for either K1 or UV5 RNA without *Taq* I digestion (Fig. 6A). Although enzyme digestion turned out not to be necessary for quantitative RT-PCR, it did reduce nonspecific background and increased the signal to noise ratio (Fig. 6A).

It was not possible to detect exon-deleted mRNA products after nine cycles of the first round of PCR, even with radiolabeling.

DISCUSSION

Correlation of nonsense mutation with exon-skipping is based on a PCR artifact

We now are able to attribute the association of nonsense mutation with exon-skipping for the *hprt* gene of CHO cells (illustrated in Fig. 2A) to an artifact of the RT-PCR method used. Using a standard, preparative RT-PCR protocol, the amplification of minor *hprt* mRNA species is suppressed both by the presence of an abundant amount of full-length mRNA and by the conditions of the PCR reaction. This produces a false negative result for parental lines and missense mutants, which have mRNA of normal abundance. When the amount of cellular full-length mRNA is reduced so that the exon-deleted species are 2% or greater of the full-length mRNA, as is the case for many nonsense mutants, the suppression is reduced and minor, exon-deleted species become detectable.

The use of a modified RT-PCR protocol (quantitative protocol) allowed us to nearly eliminate this suppressive effect and thus make a more accurate assessment of the levels of minor exon-deleted RNA species. Using this protocol, we found that exon-deleted RNA species were present in wild-type parental cells and did not, in general, increase in nonsense mutants. These results support the idea of relative enrichment (described as a "proposal" in Maquat, 1995): that exon-deleted molecules are detected by RT-PCR of RNA from nonsense mutants because they are increased in abundance relative to full-length mRNA, not because they are actually increased in abundance in the cell.

We found several factors that affected suppression of the amplification of minor, exon-deleted mRNA species by our preparative RT-PCR protocol. Suppression was reduced by the use of a more stable primer (the T_m of primer 221 is 8 °C higher than 215) at a nested position, dilution of the input RNA, and reduction of the number of PCR cycles. The single largest contributor to suppressing the amplification of exon-deleted cDNA species was abundant full-length mRNA.

The mechanism that leads to detection of exon-deleted products only when their concentration is $\geq$ 2% of normally spliced mRNA may be related to PCR artifacts that have already been described. The factors mentioned above that reduced suppression of the amplification of exon-deleted species are factors that could reduce a reannealing reaction. The $C_o t$ effect results in a relative loss of abundant species because the reannealing (rehybridization) of major species competes with amplification (Mathieu-Daudé et al., 1996). We observed this phenomenon when the quantitative RT-PCR was conducted employing the concentration of RNA used in the preparative RT-PCR protocol (Fig. 4B). However, if the major species reannealed with the minor species (heteroduplex formation) under our preparative RT-PCR conditions, the minor species could, in effect, be removed from the amplification reaction at low relative abundance. A more stable primer could speed replication of one strand and reduce its ability to reanneal. The primers used in the final PCR amplification of the quantitative protocol (221 and C7L, Fig. 4) also reduce the amount of sequence common to both the full-length and exon-deleted species (Fig. 2B); this could explain why the exon-deleted species were quantitative in Figure 4C. Even abundant species can be lost in PCR if they are GC rich in the presence of salt, but can be recovered by agents that destabilize DNA duplexes (Weissensteiner & Lanchbury, 1996). This suggests that species that do not completely melt within 1 min at 94 °C (the same conditions as our melting step) can be preferentially lost. Heteroduplexes between full-length and exon-deleted species amplified with primers for the preparative PCR protocol (215 and 216) may have secondary structures that slow their melting. Exon-deleted species are only slightly elevated in GC content relative to full-length species (1–3%) using primers 215 and 216.

Abundance of *hprt* mRNA species in mutant cell lines

Besides the nonsense-mediated effects on mRNA abundance described in the Introduction, base pair substitutions, without regard to their being nonsense or missense mutations, can cause exon-skipping and alter the concentrations of particular mRNA species due to structural effects on splice-site selection (Steingrimmsdottir et al., 1992; Belgrader & Maquat, 1994). Consideration of the quantitative RT-PCR data presented in Table 1 indicates that most concentrations of the exon-deleted *hprt* species formed in our mutant collection can be explained by either nonsense-mediated or structural effects.

Nonsense-mediated effects on the abundance of minor *hprt* mRNA species

Our previous work shows that the effect of nonsense mutation on full-length *hprt* mRNA abundance begins somewhere between 75 and 118 bases from the initial

AUG (Manjanatha et al., 1994; Fig. 2A). Several of the exon-deleted species of Table 1 still contain a nonsense mutation because the mutation was outside the deleted exons. The number of bases between the initial AUG and the first nonsense codon encountered in the deleted species is given in the table next to the quantitative value for each species (except for exon 2 deletions, explained next). Exons 2 and 3, exons 2–4, exon 4, and exon 5 deletions are in-frame; an exon 2 or 3 deletion is out-of-frame.

The exon 2-deleted species, which retained all nonsense mutations that were located in exons 3–6, was of normal abundance for most mutants. This is consistent with the fact that the translated portion of exon 1 is short (27 bases) and the exon 2 deletion is out-of-frame, producing a stop codon in the second codon of exon 3. Thus, for this species, chain termination occurs early in the message (base 33), where Figure 2A suggests there is no effect on *hprt* mRNA abundance.

The lack of the exon 2-deleted mRNA in some mutants with mutations in exon 4 was attributed (see Results) to the lack of correct splicing of exon 4. However, this species was also 20-fold less than normal in mutant 71-2, which had a nonsense mutation close to the 5′ end of exon 3. This can be explained by the nature of the mutation, which occurs in the same codon of exon 3 that becomes a stop codon in an exon 2-deleted transcript. Although the 71-2 mutation creates nonsense in the full-length transcript, it changes the first stop codon in the exon 2-deleted mRNA to a sense codon. Consequently, translation of the exon 2-deleted species with this mutation does not terminate after 33 bases, but continues to 109 bases before reaching a stop codon. This is in the borderline region for an effect on abundance and was, apparently, too far for normal abundance for this species.

There were two exceptions to the generality that *hprt* mRNA abundance is reduced when peptide termination occurs after 100 bases. Mutant 282-6B, with a nonsense mutation in exon 6, had little reduction in the abundance of the exon 2–4-deleted species, which contained a nonsense codon after 109 bases, or of the exon 2 and 3-deleted species, which contained a nonsense codon after 175 bases (Table 1). This mutation does not appear to lie beyond the coding region sensitive to nonsense-mediated effects on mRNA abundance because another nonsense codon that was 28 bases downstream (caused by a frameshift in mutant 240-9) nearly eliminated these exon-deleted species. In contrast to the minimal effect on mRNA abundance in mutant 282-6B, the exon 6 nonsense mutation in mutant 282-4B was located only 64 and 130 bases into the coding region of the exon 2–4- and 2- and 3-deleted mRNAs, and this mutant had a severe reduction of these exon-deleted species. For this severe effect, the nonsense codon was closer to the 5′ end of the coding sequence than expected because a deletion producing a nonsense codon at 75 bases had little effect on mRNA abundance (Fig. 1A; Manjanatha et al., 1994). Exon 6 is approaching the boundary of the effect on full-sized mRNA abundance, and it may be that the boundary region confers some site specificity. However, these exceptions are not understood.

Structural effects of exonic mutations on exon splicing and the abundance of minor *hprt* mRNA species

Mutant 237-1, with a missense mutation in exon 2, was the only missense mutant in our collection that contained exon-deleted mRNAs by our preparative RT-PCR protocol (Fig. 1A, M; Fig. 2). Quantitative RT-PCR indicates that mutant 237-1 had a 30-fold increase in the exon 2-deleted species (Table 1). The increase in this mRNA was intermediate between the sixfold increase in mutant 240-5 with a nonsense mutation adjacent to that in 237-1 and the 2,000-fold increase in mutant 264-0 with an exon 2 donor site deletion. This argues strongly that this missense mutation, which is 16 bp from the 3′ end of exon 2, affected splicing of exon 2 by its structural change. The sixfold increase associated with the nonsense mutation could have been caused by a modest structural effect of the same type.

Our conclusion that exon 2 mutations are acting through a structural effect on splice site recognition is strengthened by the work of Hennig et al. (1995). These authors propose a structural model for skipping of exon 2 in *hprt* mRNA of Chinese hamster V-79 cells based on a stem-loop structure that sequesters the exon 2 donor site. Mutations that stabilize the structure result in aberrant splicing. This structure not only accommodates the effects of our nonsense and missense mutations at positions 118 and 119 (mutants 240-5 and 237-1), but also another missense mutation at position 83, which was associated with the same minor, exon-deleted products by RT-PCR. This missense mutation is 56 bases from the 5′ end of exon 2 and 52 bases from the 3′ end. Thus, it would appear that a missense mutation even in the middle of a 107-base exon can cause exon skipping.

We also attribute the efficient skipping of exon 4 found for mutants 251-7 and 282-3C to structural effects of the nonsense mutations because mutant 233-0-2UA with a missense mutation at the same nucleotide as one of the nonsense mutations (11 bp from the 5′ end of exon 4) also had skipping of exon 4 and elevated exon-deleted products. Also, another mutant (282-8A) with a nonsense mutation further removed in exon 4 had exon-deleted products and mRNA abundance typical of most nonsense mutants. Other investigators have identified another missense mutation in exon 4 of the hamster *hprt* gene associated with efficient skipping of exons 3 and 4, a unique combination for the *hprt* gene to our knowledge (mutant HU/

MNU3; Zhang & Jenssen, 1991). This mutation is 29 bp from the 3′ end of the exon.

We suggest that structural effects caused by exonic mutation may also be the mechanism of action of the single nonsense mutation of the fibrillin gene that causes exon skipping, which is 26 bases from the end of its exon.

Donor site mutation effects on abundance of *hprt* mRNA species

The exon 5 nonsense and donor site mutation of mutant 240-7 was associated with unusual effects on mRNA abundance. The exon 5 deleted species was the most abundant species at 3% of the normal full-length mRNA abundance, even though it contained no nonsense mutation. The exon 2–4-deleted species was of normal abundance for that species even with the exon 5 nonsense mutation and greatly exceeded the exon 2–5-deleted species (in-frame deletion) in abundance. These results can be explained by assuming that the 3% abundance of the exon 5-deleted species is the amount of exon 5 skipping that occurred for all species, because this species had no nonsense codon and should have normal stability. The mutation is in the −3 position of the donor site, which is less well conserved and not included in the scoring system of consensus site strength of Shapiro and Senapathy (1987). Even with the mutation, this donor site still has an optimum score by this system for donor site strength (Valentine & Heflich, 1995). The full-length species was presumably reduced in abundance to less than 3% because of nonsense-mediated effects on abundance, making the exon 5-deleted species the major species. The second most abundant species, deletion of exons 2–4 (in-frame deletion), terminates translation after 43 bases at the exon 5 mutation, probably too soon to have an effect on mRNA abundance. The mRNA with deletion of exons 2 and 3 (in-frame deletion) may have shortened the distance to the exon 5 nonsense codon (109 bases, Table 1) sufficiently to eliminate or reduce the nonsense-mediated effect on abundance for this species.

Conclusions

Our data indicate that most nonsense mutations in the *hprt* gene of CHO cells that are associated with exon-skipping do not actually increase the normal abundance of exon-deleted mRNA species. Exon-deleted mRNAs are detected by a preparative RT-PCR protocol because they are relatively enriched when the nonsense mutation reduces the abundance of full-length mRNA. Because wild-type parental cells have abundant full-length mRNA and missense mutations do not reduce that abundance substantially, this protocol does not detect exon-deleted species for them. Various conditions of the RT-PCR allowed the full-length mRNA to suppress the amplification of the exon-deleted mRNAs.

A few nonsense mutations were associated with an increased abundance of exon-deleted mRNA. We attribute these results to structural effects of the mutations on splice site selection because we saw similar results with missense mutations at the same or nearby base. The possibility of exonic mutations affecting splice site selection should be considered seriously in the interpretation of occasional nonsense mutations associated with exon skipping for other genes.

MATERIALS AND METHODS

Cell lines

Cell lines and mutants are described in Valentine and Heflich (1995). Hamster *hprt* cDNA cloned in pBR322 (plasmid pHPT20; Brennand et al., 1983) was obtained from an *Escherichia coli* strain (ATCC #37430). pHPT20 includes the entire coding region of the *hprt* gene, but does not include the sequence for primer 215 (cDNA position −88 to −69; numbered from initial AUG, Konecki et al., 1982). It does include the sequence for primer 221 (−25 to −6). DNA for amplification was prepared by taking the supernatant from a colony boiled in sterile water (Valentine et al., 1994).

PCR primers

First-round *hprt* amplification

CHO *hprt* primers (positions shown in Fig. 2B) used for first-round amplification were either 215 (T_m = 55.2 °C) in Figures 2 and 6 or 221 (T_m = 63.5 °C) in Figures 3, 4, 5, and 6 for the upper primer and 216 (T_m = 50.2 °C) for the lower primer. They are from Newton et al. (1992b), except that the sequence of primer 216 is 5′-AAGCAGATGGCTGCAGAACT-3′. The length of the 215–216 fragment is 838 bp (Fig. 1).

Second-round *hprt* amplification

Second-round primers (positions shown in Fig. 2B) were 221 (Newton et al., 1992b) and C7L (5′-CCAACACTTCGAGAG GTCCTTTTC-3′; cDNA position 518–495; T_m = 55.9 °C) and PCR amplification using them produced a 543-bp fragment (Fig. 3). The *Taq* I site of exon 7 is underlined. Primer C7L was selected with the software program OLIGO™ (National Biosciences, Plymouth, Minnesota) from the CHO *hprt* cDNA sequence of Konecki et al. (1982) to prime outside exons 2 and 6 after *Taq* I restriction enzyme digestion. The 5′ end of primer C7L is not present in the PCR target after *Taq* I digestion, but 13 bp of the 3′ end of the primer were sufficient for priming in the second round of PCR. Some nonspecific priming was seen with C7L; the seven 3′ nucleotides of the primer are complementary to the sequence at positions 97–103 in exon 2 and produced a fragment of 145 bp with primer 221 when used in a 30-cycle PCR.

aprt Amplification

For quantitative RT-PCR, *aprt* primers were added to both rounds of amplification at the same concentration as the *hprt* primers. They were selected using OLIGO™ from the CHO *aprt* sequence of de Boer et al. (1989) to be inside *Taq* I restriction enzyme sites. Primers for the first round of amplification were A193U (5′-GACTCCAGGGGATTCTTGTTTG-3′; position 193–214) and A283L (5′-ATAGGAGGCTGACACT GTGGG-3′; position 303–283). Primers for the second round were A193U and A253L (5′-CCTCGCTTCCGGATGAG-3′; position 269–253). The first product was 111 bp long and the second product was 77 bp.

RNA extraction

RNA from 35–75 × 10^6 cells was isolated by the method of Chomczynski and Sacchi (1987) with the exception that 5% 2-mercaptoethanol was used instead of 0.7%. The yield of RNA was ~400 μg (~1 μg/μL).

Preparative RT-PCR protocol

The conditions for preparative RT-PCR have been described previously (Newton et al., 1992a), except they were scaled up twofold. The RT reaction contained 1 μg of input RNA based on A_{260} and was conducted in a volume of 20 μL. For the PCR, 80 μL of PCR mix was added to the RT reaction for a final volume of 100 μL. Cycling conditions were 1 min at 94 °C, 2 min at 60 °C, and 3 min at 72 °C for 30 cycles, followed by 7 min at 72 °C. Routine detection of preparative RT-PCR products was accomplished by electrophoresis on a 1% agarose gel containing 0.5 μg/mL ethidium bromide and photography using a UV-transilluminator.

Reamplification after restriction enzyme digestion of pooled RT-PCR products

In order to detect minor mRNA species by RT-PCR (Fig. 3), multiple reactions were conducted by the preparative protocol, modified by substituting primer 221 for 215. Reaction mixtures from these amplifications were pooled and the products were purified with a Centricon 100 filtration apparatus (Amicon, Beverly, Massachusetts). Approximately 100 ng of the PCR products were digested in a 20-μL reaction volume with 20U of *Hae* III or *Taq* I (GIBCO-BRL, Gaithersburg, Maryland) for 2 h at 37 °C or 65 °C, respectively. The reaction mixtures were diluted 1/100 and 2 μL was reamplified in a 100-μL reaction using primers 221 and C7L and the same thermocycling conditions used as for the first amplification. Eight microliters of each reaction mixture was applied to 6% acrylamide TBE gels (Novex, San Diego, California).

DNA sequencing

Bands cut from ethidium bromide-stained acrylamide gels were eluted in 0.5 M ammonium acetate, 10 mM magnesium acetate, 1.0 mM EDTA, and 0.1% SDS overnight with rocking at 37 °C. The DNA was concentrated by ethanol precipitation and sequenced by dideoxy cycle sequencing using an automated ABI 373A sequencer as described previously (Valentine & Heflich, 1995). The sequence of Chinese hamster lines K1, UV5, and V79 differs from the sequence of Konecki et al. (1982) by a C at position 464 instead of T. All of our parent strains and mutants also had C at this position.

Quantitative RT-PCR

The methods were adapted from the preparative RT-PCR protocol as follows. The concentration of RNA from the parental line K1 was 1.2 μg/μL as determined by A_{260}; all other samples were normalized to this concentration based on 28S RNA amount. In order to quantitate 28S RNA, 2 μg of all RNA samples were electrophoresed on a 2% formaldehyde, 1% agarose gel in 0.05 M HEPES, pH 7.8, 5 mM EDTA buffer. The gel was stained with SYBR™ Green II (FMC, Rockland, Maine) and visualized with a FluorImager SI (Molecular Dynamics, Sunnyvale, California). Quantitation of the 28S bands was performed with ImageQuant™ software.

The first round of RT-PCR was performed using the conditions described for the preparative protocol except that only nine cycles were used and that the *hprt* primers were 221 and 216 and *aprt* primers were added (PCR primers above). Six microliters of this mixture was diluted into a 20-μL *Taq* I restriction enzyme digest (3.3-fold dilution) and digested for 2 h at 65 °C. If the full-length mRNA or the relative amount of exon 2–4-deleted to full-length species was being evaluated, a mock digestion was performed containing water for enzyme. After a 100-fold dilution, 5 μL were amplified in a 50-μL PCR reaction with primers 221 and C7L (above) for 26 cycles using the same cycling conditions as the first round. This reaction contained 0.4 μCi [α-^{32}P] dATP (Chen & Chasin, 1993; 3,000 Ci/mmol for the dilution series; 6,000 Ci/mmol for all subsequent reactions with 250 ng RNA). Nine microliters of this reaction mixture was electrophoresed on a 6% acrylamide gel. The gel was dried and exposed to a phosphor storage screen for 3–21 h. Radioactivity was detected using a Molecular Dynamics PhosphorImager. Quantitation of the bands was performed with ImageQuant™ software. Three different quantitations for each band were averaged together. Images were exported for graphics additions with Adobe Illustrator™ (Adobe, Mountain View, California).

In order to establish the linearity of the amplification, twofold dilutions of K1 RNA (maximum of 1 μg per reaction) were analyzed by this protocol. After the serial dilutions were quantitated, a fourfold dilution of all RNA samples was chosen as the concentration for all further work (~250 ng RNA/100 μL reaction).

Mixing experiments

The preparative and quantitative RT-PCR protocols were used as well as stepwise variations between the two as specified in the legend to Figure 6. RNA from two different samples was used in some amplifications without changing the total volume of the reaction mixture. The same amount of RNA added to reactions conducted with individual RNA samples was added to the mixtures.

Quantitative comparisons between mutants and parental lines

Corrections were applied to the *aprt* measurements because two distinct linear ranges could be distinguished for the relationship between *aprt* amplification and RNA concentration. Figure 4A shows a linear relationship with a *y*-intercept of 33% when the product was 65% or above the 250 ng level. Therefore, for *aprt* values of mutants that were ≥ 65% of the parent strain's value, 33% of the parent *aprt* value was subtracted from the mutant value in order to bring the line through the origin and make the % *aprt* product formed proportional to the input RNA. The *aprt* values from the mutant and the parent were then expressed as a ratio and used to normalize the values for exon-deleted bands. A few mutants had *aprt* values below 65% of the parent strain's value; for these, the correction was done graphically from Figure 4A, instead of arithmetically. For example, if an *aprt* value for a mutant was 45% of the value from the parent strain, a value of 84 ng RNA was read from the graph (Fig. 4A). This value was divided by 250 ng RNA, which was the standard amount used for the parental samples, to arrive at the normalizing ratio. This allowed a comparison between the two linear parts of the dose-response curve.

The full-length species also showed a dual linearity that was less pronounced (Fig. 4B). Because the ratio of full-length species to *aprt* standard was constant (within 10%) over the range of RNA amounts up to 500 ng, no further correction was made for the quantitation of the full-length species after the correction for the *aprt* standard. We considered that the comparisons were accurate within twofold.

ACKNOWLEDGMENTS

We are grateful to Lawrence A. Chasin for informative and helpful discussions and to Barbara Parsons for her thoughtful reading of the manuscript.

Received April 26, 1996; returned for revision June 10, 1996; revised manuscript received March 4, 1997

REFERENCES

Bach G, Moskowitz SM, Tieu PT, Matynia A, Neufeld EF. 1993. Molecular analysis of Hurler syndrome in Druze and Muslim Arab patients in Israel: Multiple allelic mutations of the *IDUA* gene in a small geographic area. *Am J Human Genetics 53*:330–338.

Belgrader P, Cheng J, Zhou X, Stephenson LS, Maquat LE. 1994. Mammalian nonsense codons can be *cis* effectors of nuclear mRNA half-life. *Mol Cell Biol 14*:8219–8228.

Belgrader P, Maquat LE. 1994. Nonsense but not missense mutations can decrease the abundance of nuclear mRNA for the mouse major urinary protein, while both types of mutations can facilitate exon skipping. *Mol Cell Biol 14*:6326–6336.

Brennand J, Konecki DS, Caskey CT. 1983. Expression of human and Chinese hamster hypoxanthine-guanine phosphoribosyltransferase cDNA recombinants in cultured Lesch-Nyhan and Chinese hamster fibroblasts. *J Biol Chem 258*:9593–9596.

Caponigro G, Parker R. 1996. Mechanisms and control of mRNA turnover in *Saccharomyces cerevisiae*. *Microbiol Rev 60*:233–249.

Chasin LA, Urlaub G, Mitchell P, Ciudad C, Barth J, Carothers AM, Steigerwalt T, Brunberger D. 1990. RNA processing mutants at the dihydrofolate reductase locus in Chinese hamster ovary cells. In: Mendelsohn ML, Albertini RJ, eds. *Mutation and the environment, part A. Basic mechanisms*. New York: Wiley-Liss. pp 295–304.

Chen IT, Chasin LA. 1993. Direct selection for mutations affecting specific splice sites in a hamster dihydrofolate reductase minigene. *Mol Cell Biol 13*:289–300.

Cheng J, Fogel-Petrovic M, Maquat LE. 1990. Translation to near the distal end of the penultimate exon is required for normal levels of spliced triosephosphate isomerase mRNA. *Mol Cell Biol 10*:5215–5225.

Chomczynski P, Sacchi N. 1987. Single-step method of RNA isolation by acid guanidinium thiocyanate-phenol-chloroform extraction. *Anal Biochem 162*:156–159.

Cole J, Skopek TR. 1994. International Commission for Protection Against Environmental Mutagen and Carcinogens. Working paper no. 3. Somatic mutant frequency, mutation rates and mutational spectra in the human population in vivo. *Mutation Res 304*:33–105.

de Boer JG, Drobetsky EA, Grosovsky AJ, Mazur M, Glickman BW. 1989. The Chinese hamster *aprt* gene as a mutational target. Its sequence and an analysis of direct and inverted repeats. *Mutation Res 226*:239–244.

Dietz HC, Kendzior RJ Jr. 1994. Maintenance of an open reading frame as an additional level of scrutiny during splice site selection. *Nature Genetics 8*:183–188.

Dietz HC, Pyeritz RE. 1995. Mutations in the human gene for fibrillin-1 (*FBN1*) in the Marfan syndrome and related disorders. *Human Mol Genetics 4*:1799–1809.

Dietz HC, Valle D, Francomano CA, Kendzior RJ Jr, Pyeritz RE, Cutting GR. 1993. The skipping of constitutive exons in vivo induced by nonsense mutations. *Science 259*:680–683.

Gibson RA, Hajianpour A, Murer-Orlando M, Buchwald M, Mathew CG. 1993. A nonsense mutation and exon skipping in the Fanconi anaemia group C gene. *Human Mol Genetics 2*:797–799.

Hennig E, Conney AH, Wei SJC. 1995. Characterization of *hprt* splicing mutations induced by the ultimate carcinogenic metabolite of benzo[α]pyrene in Chinese hamster V-79 cells. *Cancer Res 55*: 1550–1558.

Hull J, Shackleton S, Harris A. 1994. The stop mutation R553X in the CFTR gene results in exon-skipping. *Genomics 19*:362–717.

Jarolim P, Rubin HL, Brabec V, Palek J. 1995. A nonsense mutation 1669Glu → Ter within the regulatory domain of human erythroid ankyrin leads to a selective deficiency of the major ankyrin isoform (band 2.1) and a phenotype of autosomal dominant hereditary spherocytosis. *J Clin Invest 95*:941–947.

Kessler O, Chasin LA. 1996. Effects of nonsense mutations on nuclear and cytoplasmic adenine phosphoribosyltransferase RNA. *Mol Cell Biol 16*:4426–4435.

Konecki DS, Brennand J, Fuscoe JC, Caskey CT, Chinault AC. 1982. Hypoxanthine-guanine phosphoribosyltransferase genes of mouse and Chinese hamster: Construction and sequence analysis of cDNA recombinants. *Nucleic Acids Res 10*:6763–6775.

Manjanatha MG, Lindsey LA, Mittelstaedt RA, Heflich RH. 1994. Low *hprt* levels and multiple *hprt* mRNA species in 6-thioguanine-resistant Chinese hamster cell mutants possessing nonsense mutations. *Mutation Res 308*:65–75.

Maquat L. 1995. When cells stop making sense: Effects of nonsense codons on RNA metabolism in vertebrate cells. *RNA 1*:453–465.

Maquat L. 1996. Defects in RNA splicing and the consequence of shortened translational reading frames. *Am J Human Genetics 59*:279–286.

Mathieu-Daudé F, Welsh J, Vogt T, McClelland M. 1996. DNA rehybridization during PCR: The "C_0t effect" and its consequences. *Nucleic Acids Res 24*:2080–2086.

Naylor JA, Green PM, Rizza CR, Giannelli F. 1993. Analysis of factor VIII mRNA reveals defects in everyone of 28 haemophilia A patients. *Human Mol Genetics 2*:11–17.

Newton RK, Mittelstaedt RA, Heflich RH. 1992a. Analysis of solvent control and 1-nitrosopyrene-induced Chinese hamster ovary cell mutants by Southern and Northern blots and the polymerase chain reaction. *Environ Mol Mutagenesis 19*:147–155.

Newton RK, Mittelstaedt RA, Manjanatha MG, Heflich RH. 1992b. DNA sequence analysis of 1-nitrosopyrene-induced mutations in the *hprt* gene of Chinese hamster ovary cells. *Carcinogenesis 13*:819–825.

Shapiro MB, Senapathy R. 1987. RNA splice junctions of different classes of eukaryotes: Sequence statistics and functional implications in gene expression. *Nucleic Acids Res 15*:7155–7174.

Steingrimmsdottir H, Rowley G, Dorado G, Cole J, Lehmann AR. 1992. Mutations which alter splicing in the human hypoxanthine-guanine phosphoribosyltransferase gene. *Nucleic Acids Res 20*: 1201–1208.

Valentine CR, Heflich RH. 1995. Genomic DNA sequencing of mRNA splicing mutants in the *hprt* gene of Chinese hamster ovary cells. *Environ Mol Mutagenesis 25*:85–96.

Valentine CR, Heinrich MJ, Chissoe SL, Roe BA. 1994. DNA sequence of direct repeats of the *sul* I gene of plasmid pSa. *Plasmid 32*:222–227.

Weissensteiner T, Lanchbury JS. 1996. Strategy for controlling preferential amplification and avoiding false negatives in PCR typing. *BioTechniques 21*:1102–1108.

Will K, Dörk T, Stuhrmann M, von der Hardt H, Ellemunter H, Tümmler B, Schmidtke J. 1995. Transcript analysis of CFTR nonsense mutations in lymphocytes and nasal epithelial cells from cystic fibrosis patients. *Human Mutation 5*:210–220.

Zhang L-H, Jenssen D. 1991. Site specificity of *N*-methyl-*N*-nitrosourea-induced transition mutations in the *hprt* gene. *Carcinogenesis 12*:1903–1909.